Catalysis Science & Technology

Accepted Manuscript

ROYAL SOCIETY OF CHEMISTRY

www.rsc.org/catalysis

Journal Name

RSCPublishing

ARTICLE

Asymmetric hydrogenation by $RuCl_2$(*R*-Binap)$(dmf)_n$ encapsulated in silica-based nanoreactors

Cite this: DOI: 10.1039/x0xx00000x

Juan Peng,[a,b] Xuefeng Wang,[a] Xiaoming Zhang,[a,b] Shiyang Bai,[a] Yaopeng Zhao,[a] Can Li [a*] and Qihua Yang [a*]

Received 00th January 2012,
Accepted 00th January 2012

DOI: 10.1039/x0xx00000x

www.rsc.org/

The Noyori catalyst $RuCl_2$(*R*-Binap)$(dmf)_n$ has been successfully encapsulated in C-FDU-12 by using the active chlorosilane Ph_2Cl_2Si as the silylation reagent. ^{31}P-NMR results show that there is no strong interaction between the molecular catalyst and the solid support, thus the encapsulated molecular catalyst could move freely in the nanoreactor during the catalyticprocess. The solid catalyst exhibits high activity and enantioselectivity for the asymmetric hydrogenation of a series of β-keto esters due to the preserved intrinsic property of $RuCl_2$(*R*-Binap)$(dmf)_n$ encapsulated in the nanoreactor. The solid catalyst could be recycled by simple filtration and be reused for at least four times.

Introduction

Asymmetric catalysis is one of the most efficient approaches for the production of chiral chemicals. In the past decades, big progresses have been made for homogeneous asymmetric catalysis. Versatile efficient asymmetric catalytic systems have been developed for the synthesis of various enantiomers which are important in both fine-chemical and pharmaceutical industries. [1-5] From the view point of industrial application, it is desirable for the production of chiral compounds through heterogeneous asymmetric catalytic approach due to its overwhelming advantages in recycling and reuse of the expensive homogeneous asymmetric catalysts, easy purification of the products and convenient manipulation for large scale production.

However, heterogeneous asymmetric catalysts which are often prepared by simple immobilization of homogeneous asymmetric catalysts onto solid supports always face the problems of low enantioselectivity and catalytic activity. [6,7] This is partly because the molecular catalysts lose their mobility after immobilization, which may alter their intrinsic properties. Great efforts have been made to try to keep the intrinsic properties of molecular catalysts after immobilization, for example, encapsulating the metal complex catalyst in zeolite through a "ship-in-bottle" method. [8-10] Unfortunately, the small pore size of zeolites and the uncontrollable coordination process within pores have restricted its application for more complicated catalysts. Recently, our group has developed an efficient strategy for encapsulating molecular catalysts in the silica-based nanoreactors with cage-like porous structure, such as SBA-16 and FDU-12, by post-modification of the pore entrance through a silylation method. With this method, several kinds of metal complex catalysts, such as Co(Salen), [11-13] VO(Salen), [14] Fe(Salan), [15] Cr(Salen), [16] Ru(Ts-DPEN) [17] and $(Binolate)_2Ti$ [18] have been successfully trapped in the nanocages of mesoporous materials. It has also been demonstrated that the encapsulated molecules could move freely in the nanoreactor based on the ^{31}P-NMR characterizations using BINAPO (2,2'-bis(diphenylphosphinooxide)-1,1'-binaphthyl) as the model molecule. [13] The catalytic performance of the encapsulated molecular catalysts is comparable to and in some cases even higher than the homogeneous counterparts.

Our previous encapsulation method always required organic base, such as pyridine, as a silylation catalyst during the silylation process for reducing the pore entrance size. However, due to its strong coordination ability, pyridine may deteriorate some metal complexes. It is therefore desirable to develop new methods for the encapsulation of the special types of catalysts, for example, $RuCl_2$(*R*-Binap)$(dmf)_n$ (abbreviated as Ru-(*R*-Binap) in the following paragraphs, as for the structural formula, $RuCl_2$(*R*-Binap)$(dmf)_2$ (n=2) is taken as the representative), which has been widely used in asymmetric hydrogenation after being reported by Noyori and Takaya in 1980. [19] Ru-(*R*-Binap) is air sensitive and losses its catalytic activity in the presence of pyridine. Many efforts have been made to immobilize Binap onto different kinds of supports, such as zirconium phosphonate, [20,21] Fe_3O_4, [22,23] PMOs, [24] graphite oxide, [25] polymers, [26] ionic liquids, [27-29] etc., however, the immobilization of Ru-(*R*-Binap) through the non-covalent interaction has rarely been reported. Herein, we describe a new method for encapsulating this organic base sensitive catalyst in the nanocages of mesoporous silicas C-FDU-12 without deteriorating its activity. According to the characterization results of nitrogen adsorption-desorption analysis, XRD and TEM, the ordered mesoporous structure of the cage-like meterial is maintained after the encapsulation of Ru-(*R*-Binap). Furthermore, ^{31}P-NMR spectroscopic studies show that the encapsulated Ru-(*R*-Binap) could move freely in the nanocages, which was seldom reported by other immobilization methods. To evaluate the

catalytic performance of Ru-(*R*-Binap)@C-FDU-12, the asymmetric hydrogenation of β-keto esters is chosen as the model reaction. The influence of the loading amount of Ru-(*R*-Binap) on the catalytic performance of Ru-(*R*-Binap)@C-FDU-12 and the cycling stability of Ru-(*R*-Binap)@C-FDU-12 are also investigated.

Results and Discussion

Encapsulation of Ru-(*R*-Binap) complex in the nanocage of C-FDU-12

As illustrated in Scheme 1, Ru-(*R*-Binap) is first introduced into the nanocage of C-FDU-12 (obtained by carbonization of the as-made FDU-12 at 550°C under the nitrogen atmosphere for 6 h, the carbon content is 4.8 wt%, Figure 1b) under vacuum. Then the pore entrance size is reduced using Ph_2Cl_2Si as the silylation reagent at room temperature under vacuum. After being thoroughly washed with dichloromethane in glove box, the solid catalyst, Ru-(*R*-Binap)@C-FDU-12, was obtained. In this case, we choose very active chlorosilane Ph_2Cl_2Si [30] instead of alkoxysilanes as silylation reagent, thus the silylation could be performed at room temperature without any silylation catalysts. This will benefit to keep the intrinsic properties of Ru-(*R*-Binap) during the encapsulation process.

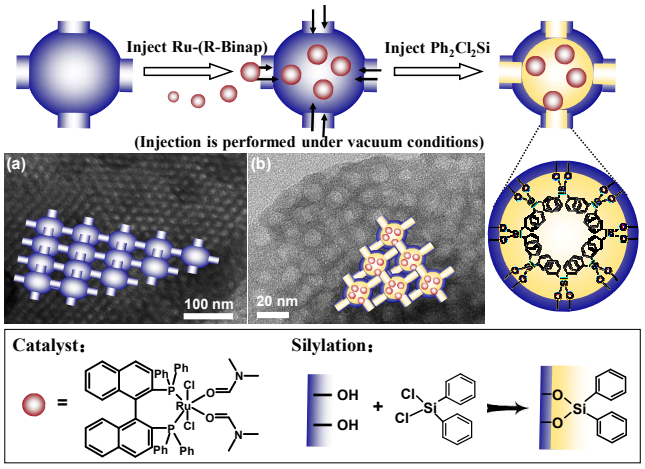

Scheme 1. Schematic illustration of encapsulating Ru-(*R*-Binap) in the nanocage of C-FDU-12 and TEM images of C-FDU-12 (a) before and (b) after encapsulation of Ru-(*R*-Binap).

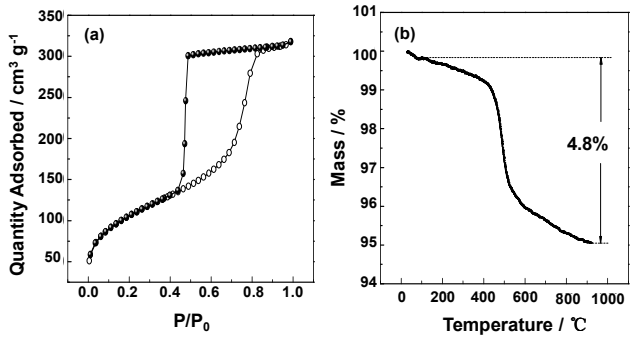

Figure 1. (a) The N_2 sorption isotherm and (b) TG analysis of C-FDU-12.

FT-IR spectra of Ru-(*R*-Binap) and Ru-(*R*-Binap)@C-FDU-12 are presented in Figure 2. Ru-(*R*-Binap)@C-FDU-12 displays the characteristic vibration bands of Ru-(*R*-Binap) at 3050 cm^{-1}, 810 cm^{-1}, 743 cm^{-1}, 697 cm^{-1} for C (naphthalene)-H, and 1434 cm^{-1} for P-C (aryl). The UV-vis diffused reflectance spectrum of Ru-(*R*-Binap)@C-FDU-12 clearly shows the bands at 338 nm, similar to that of Ru-(*R*-Binap) dissolved in CH_2Cl_2 (Figure S3). The results of FT-IR and UV-vis confirm the successful encapsulation of Ru-(*R*-Binap) in the nanocage of C-FDU-12.

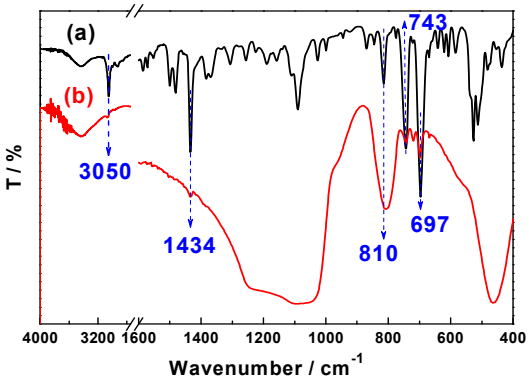

Figure 2.FT-IR spectra of (a) Ru-(*R*-Binap) and (b) Ru-(*R*-Binap)@C-FDU-12 (0.71wt% Ru).

Texture properties of Ru-(*R*-Binap)@C-FDU-12

The N_2 sorption isotherms of Ru-(*R*-Binap)@C-FDU-12 are of type IV with an H2 hysteresis loop similar to that of parent C-FDU-12, indicating that the solid catalyst still maintains the cage-like porous structure (Figure 1a and Figure 3A). In comparison with C-FDU-12, the obvious decrease in the BET surface area and cage size is observed due to the occupation of Ru-(*R*-Binap) catalyst in the nanocages (Table 1). As the content of Ru-(*R*-Binap) increases, the BET surface area and pore volume of Ru-(*R*-Binap)@C-FDU-12 decreases gradually.

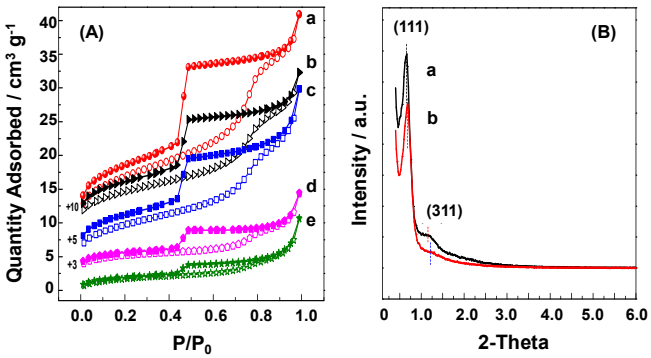

Figure 3. (A) The N_2 sorption isotherms of Ru-(*R*-Binap)@C-FDU-12 with different Ru content: (a) 0.12 wt%, (b) 0.28 wt%, (c) 0.37 wt%, (d) 0.5 wt% and (e) 0.71 wt%. (B) XRD patterns of (a) C-FDU-12 and (b) Ru-(*R*-Binap)@C-FDU-12 (0.71wt% Ru).

The XRD patterns of Ru-(*R*-Binap)@C-FDU-12 (0.71wt% Ru) exhibit two well-resolved diffraction peaks (Figure 3B), which can be indexed to the (111) and (311) reflections of afcc structure (Fm3m), [31] similar to C-FDU-12. The TEM images

also show that the ordered distribution of the mesopores of C-FDU-12 maintains invariable after the encapsulation of Ru-(*R*-Binap) (Scheme 1). The above results confirm that Ru-(*R*-Binap)@C-FDU-12 has well ordered cage-like porous structure and the encapsulation of Ru-(*R*-Binap) does not damage the porous structure of C-FDU-12.

Table 1. The textural parameters of C-FDU-12 and Ru-(*R*-Binap)@C-FDU-12 with different Ru content.

Catalysts	Ru content / wt%	S_{BET} / m^2g^{-1}	V_p/ cm^3g^{-1} [a]	Cage size / nm [b]
Ru-(*R*-Binap)@ C-FDU-12-0	0	381	0.49	9.1
Ru-(*R*-Binap)@ C-FDU-12-0.12	0.12	26.4	0.048	8.0
Ru-(*R*-Binap)@ C-FDU-12-0.28	0.28	17.9	0.034	8.0
Ru-(*R*-Binap)@ C-FDU-12-0.37	0.37	18.1	0.038	8.0
Ru-(*R*-Binap)@ C-FDU-12-0.5	0.5	8.2	0.017	8.0
Ru-(*R*-Binap)@ C-FDU-12-0.71	0.71	6.6	0.016	8.0

[a] Estimated from the amounts adsorbed at a relative pressure (P/P_0) of 0.99.
[b] The pore size distribution calculated from the N_2 adsorption branch using the BJH method.

Investigation of movement freedom of Ru-(*R*-Binap) encapsulated in C-FDU-12

In our previous work, the degree of movement freedom of the molecule encapsulated in the nanocages of mesoporoussilicas was detected using BINAPO (2,2'-bis(diphenylphosphinooxide)-1,1'-binaphthyl) as a model molecule. [13] However, the movement freedom of the real catalysts has not been detected. In this work, the movement freedom of molecular catalyst, Ru-(*R*-Binap), in the nanocages of C-FDU-12 is investigated by ^{31}P-NMR characterizations.

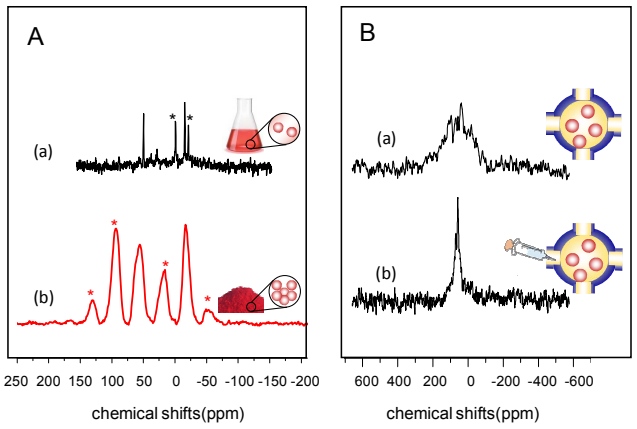

Figure 4. (A) (a) Liquid ^{31}P-NMR spectrum performed under inert atmosphere using degassed $CHCl_3$ as solvent and (b) magic-angle spinning (MAS) solid-state ^{31}P-NMR spectrum of Ru-(*R*-Binap); (B) Static ^{31}P-NMR spectra of Ru-(*R*-Binap)@C-FDU-12 (0.71wt% Ru) (a) in solid state and (b) in suspension with degassed $CHCl_3$ as solvent.

Liquid ^{31}P-NMR spectrum of Ru-(*R*-Binap) and its magic-angle spinning Solid-State ^{31}P-NMR spectrum are shown in Figure 4A. The isotropic chemical shift at 56 ppm and -16.2 ppm could be identified by magic-angle spinning (Figure 4Ab), which could be respectively assigned to the signal of Ru-(*R*-Binap) and R-Binap ligand residue (excessive *R*-Binap ligand was used for the synthesis of Ru-(*R*-Binap) according to previous report [32]). An asymmetric and broad peak was observed in the static^{31}P NMR spectrum of Ru-(*R*-Binap)@C-FDU-12 due to the chemical-shift anisotropy of the ^{31}P nucleus (Figure 4Ba). Interestingly, the static ^{31}P NMR spectrum of Ru-(*R*-Binap)@C-FDU-12 displays a sharp peak at 56 ppm in the presence of solvent (Figure 4Bb), indicating that Ru-(*R*-Binap) could move in the nanocages of C-FDU-12. The static ^{31}P-NMR spectra of Ru-(*R*-Binap)@C-FDU-12 in the presence of different amounts of solvent are summarized in Figure 5. The peak firstly appears with the presence of 20 ul $CHCl_3$, corresponding to 40 % of the cage volume filled with the solvent (according to the N_2 sorption results). As the amount of $CHCl_3$ increases, the peak at 56 ppm becomes sharper, and the intensity of the signal increases and reaches a maximum with the $CHCl_3$ amount of 50 ul, corresponding to 100 % of the cage volume filled with the solvent. It should be mentioned that the peak at -16.2 ppm which belongs to *R*-Binap could hardly be observed in the ^{31}P-NMR spectrum of Ru-(*R*-Binap)@C-FDU-12, indicating that the silylation with Ph_2Cl_2Si is very efficient and controllable for modifying the pore entrance of C-FDU-12.

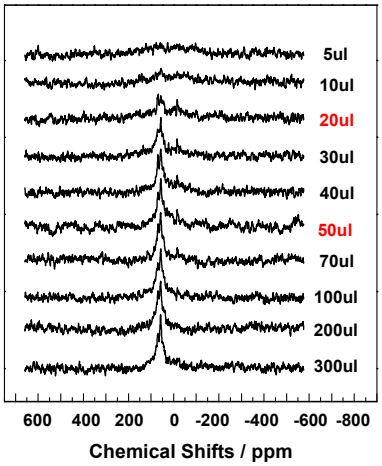

Figure 5.^{31}P-NMR spectra measured under static conditions of Ru-(*R*-Binap)@C-FDU-12 (0.71wt% Ru)in the presence of different amounts of $CHCl_3$.

The NMR spectroscopic studies further confirm that Ru-(*R*-Binap) has been successfully encapsulated in the nanocage of C-FDU-12. Moreover, the confined Ru-(*R*-Binap) can move freely in the nanocages during a liquid phase catalytic process. Thus, Ru-(*R*-Binap)@C-FDU-12 is solid catalyst as a whole, but has homogeneous properties at nanoscale.

Asymmetric hydrogenation of β-keto esters

The catalytic performance of Ru-(*R*-Binap)@C-FDU-12 is investigated in the asymmetric hydrogenation of methyl

Table 2. Asymmetric hydrogenation of methyl acetoacetate (MAA) catalyzed by Ru-(*R*-Binap)@C-FDU-12 with different Ru loadings. [a]

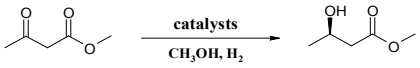

Entry	Catalysts	Number of cat.percage	S/C	TOF / h^{-1} [b]	Yield / % [c]	Ee. / % [c]
1	C-FDU-12	-	-	-	0	-
2	Ru-(*R*-Binap)	-	1000	1101	99	97.1
3	Ru-(*R*-Binap)@ C-FDU-12-0.12	7	1000	299	99	96.5
4	Ru-(*R*-Binap)@ C-FDU-12-0.12	7	2000	382	97	93.0
5	Ru-(*R*-Binap)@ C-FDU-12-0.28	16	1000	227	99	96.7
6	Ru-(*R*-Binap)@ C-FDU-12-0.37	21	1000	152	99	96.9
7	Ru-(*R*-Binap)@ C-FDU-12-0.5	28	1000	127	99	97.3
8	Ru-(*R*-Binap)@ C-FDU-12-0.71	39	1000	100	99	96.7
9	Ru-(*R*-Binap)@ C-FDU-12-0.82	45	1000	82	99	97

[a] All the reactions are carried out under a hydrogen pressure of 4 MPa in 1.0 mL methanol at 50 °C for 24 h
[b] TOFs are calculated at the initial 1h;
[c] Yield and ee values are determined by GC on a Supelco g-DEX 225 capillary column

acetoacetate. As shown in Table 2, no product is detected with only C-FDU-12, showing that C-FDU-12 is not active for this reaction. Under the same reaction conditions, Ru-(*R*-Binap)@C-FDU-12-0.12 (0.12 wt% Ru) exhibits 99% yield with 96.5% ee, which is very close to its homogeneous counterpart. The high ee of Ru-(*R*-Binap)@C-FDU-12 suggests that the current encapsulation method does not cause the damage to Ru-(*R*-Binap) during the silylation process. The TOF of Ru-(*R*-Binap) is still lower than that of the homogeneous Ru-(*R*-Binap). This is due to the mass diffusion limitation of reactants and products through the nanocages. When the S/C increases to 2000, the yield and enantioselectivity of methyl-3-hydroxybutyrate do not significantly alter any way, while the TOF value becomes a little higher, as shown in entry 4. The influence of the catalyst loading amount on the catalytic performance of Ru-(*R*-Binap)@C-FDU-12 is also investigated (Entry 3, 5-9). With the metal loading increasing from 0.12 wt% to 0.82 wt%, the molecular number of the metal complex in each cage increases from 7 to 45, and the TOF value of Ru-(*R*-Binap)@C-FDU-12 decreases from 299 h^{-1} to 82 h^{-1}, while the enantioselectivity nearly keeps the same (Figure 6). As shown in Table 1, the BET surface area and pore volume of Ru-(*R*-Binap)@C-FDU-12 decrease as the Ru-(*R*-Binap) loading increases. Thus, the decreased activity is probably due to the crowded microenvironment in the nanocages caused by the high content of Ru-(*R*-Binap), which makes the diffusion of reactants and products difficult. The maintained enantioselectivity indicates that the property of Ru-(*R*-Binap) keeps unchanged regardless of the number of the molecular catalyst encapsulated in the nanocages. Figure 7 gives the kinetic plots of the asymmetric hydrogenation of methyl acetoacetate on Ru-(*R*-Binap)@C-FDU-12 with Ru contents of 0.5 wt%. After the reaction has been carried out for 3 h, the solid catalyst is filtered off, while the filtrate is stirred under the same conditions for another 21 h. However, the yield of the product remains almost the same with that measured at 3 h, confirming that the solid catalyst actually is responsible for the catalytic reaction.

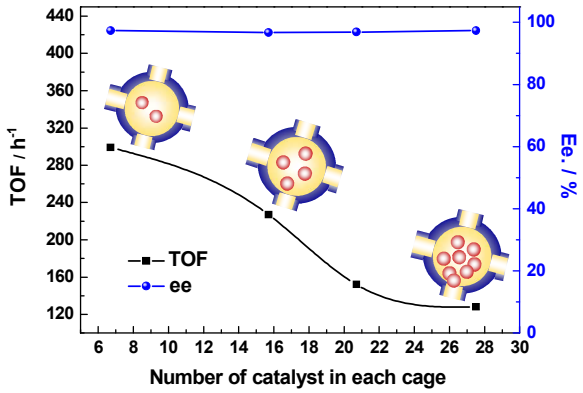

Figure 6. TOF and ee values of MAA hydrogenation in the presence of Ru-(*R*-Binap)@C-FDU-12 with different numbers of Ru-(*R*-Binap) molecules in each nanocage.

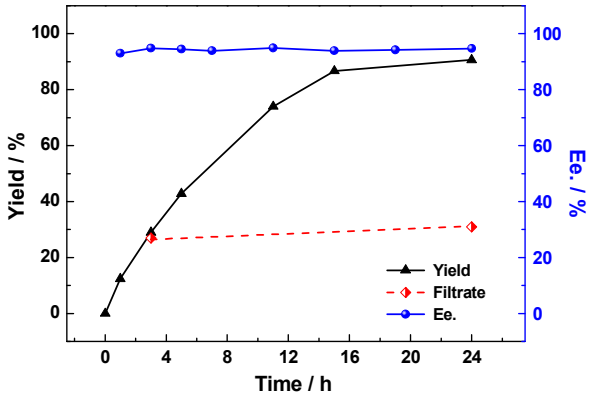

Figure 7. Kinetic plots of the asymmetric hydrogenation of methyl acetoacetate on Ru-(*R*-Binap)@C-FDU-12 with Ru contents of 0.5 wt%. The filtrate test is performed by removing the solid catalyst out of the reaction system after 3 h.

Anyway, this encapsulation method enables the precise control of the loading amount of metal complexes in the nanocages to meet different needs. For some particular asymmetric catalytic system, the number of the encapsulated metal complexes should be precisely adjusted for obtaining high activity, e.g., one molecule per nanocage for the catalyst which may be deactivated by dimer formation (such as Ir-Binap), and two molecules or above for catalysts which show the cooperative activation effect (such as CoSalen).

The encapsulated catalyst is also used to catalyze the asymmetric hydrogenation of a wide range of β-keto esters for the production of different β-hydroxy esters, which are important intermediates in the fine chemical and pharmaceutical industries. As shown in Table 3, all of these substrates can be efficiently converted into the corresponding chiral alcohol on Ru-(*R*-Binap)@C-FDU-12 with high yield (91~99%) and high enantioselectivity (87~99% ee).

Table 3.Catalytic performance of Ru-(*R*-Binap)@C-FDU-12 [a] and homogeneous Ru-(*R*-Binap) for asymmetric hydrogenation of various β-keto esters.[b]

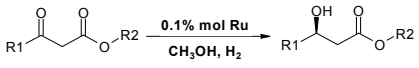

Entry	R	Yield / % [c]	Ee. / % [c]
1	R^1=R^2=Me	99 (99)	97 (97.1)
2	R^1=Et, R^2=Me	99 (98.4)	98.8 (97.7)
3	R^1=i-Pr, R^2=Me	94.2 (97.8)	99 (99)
4	R^1=t-Bu, R^2=Me	99 (99)	99 (99)
5	R^1=-CH_2-Ph, R^2=Me	99 (99)	99 (99)
6	R^1=Me, R^2=Et	99 (99)	99 (99)
7	R^1=Me, R^2=i-Pr	91 (99)	87 (97)

[a] Ru-(*R*-Binap)@C-FDU-12 with Ru content of 0.12 wt%.
[b] All the reactions are carried out under a hydrogen pressure of 4 MPa in 1.0 mL methanol at 50 °C with S:C=1000:1.
[c] The data in parentheses are for homogeneous Ru-(*R*-Binap).

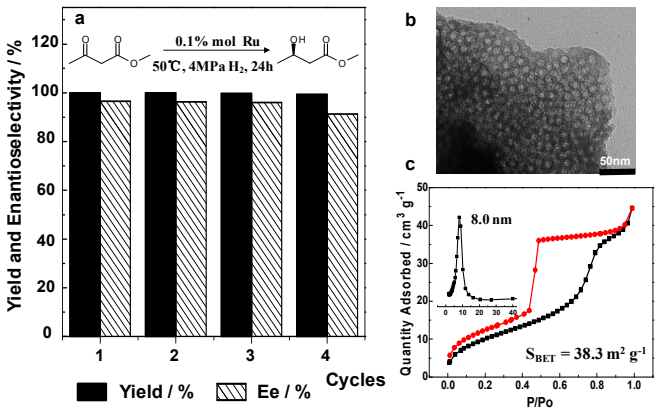

Figure 8. (a) Recycling test of Ru-(*R*-Binap)@C-FDU-12 (0.12wt% Ru) in the asymmetric hydrogenation of methyl acetoacetate, (b) TEM image and (c) N_2 sorption isotherms of Ru-(*R*-Binap)@C-FDU-12 (0.12wt% Ru) after cycling for 4 times.

Ru-(*R*-Binap)@C-FDU-12 exhibits good catalytic stability and could be easily recycled by simple filtration method. For the hydrogenation of methyl acetoacetate, the yield and enantioselectivity of the solid catalyst remains above 90% after four cycles (Figure 8a). After the first cycle, 0.98 wt% of Ru was found in the reaction filtrate by ICP analysis. While for the second cycle, the amount of the leaching species dropped down to 0.26 wt%, and little Ru species could be detected after the third cycle. The recycled solid catalyst could still maintain the mesoporous structures of the fresh Ru-(*R*-Binap)@C-FDU-12 (Figure 8b and c). The slight decrease in activity and enantioselectivity during the recycle process is considered to be partly caused by the air sensitivity of the catalytically active Ru-hydride species and partly due to the leaching of metal complexes. [20,33]

Conclusions

In summary, we have developed an efficient method for the encapsulation of organic base sensitive metal complexes in the nanocages of mesoporous silicas. With highly active chlorosilane, Ph_2Cl_2Si, as a silylation agent, the encapsulation could be performed at room temperature without any silylation catalysts. This method is proved to be available for the encapsulation of the Noyori catalyst Ru-(*R*-Binap) in the nanocages of C-FDU-12 without damaging Ru-(*R*-Binap). ^{31}P-NMR results show that the encapsulated molecular catalyst could move freely in the nanocages during a liquid phase catalytic process. Thus, the intrinsic property of Ru-(*R*-Binap) is preserved. Ru-(*R*-Binap)@C-FDU-12 exhibits excellent enantioselectivity which is comparable with its homogeneous counterpart for the asymmetric hydrogenation of β-keto esters and could be reused for at least four times. We could expect that this encapsulation strategy would be generally applicable for the design of various high-efficient nanoreactors for the production of fine chemicals and pharmaceuticals.

Experimental Section

Material information

Pluronic copolymer F127 (EO106PO70EO106) and $[RuCl_2(benzene)]_2$ were purchased from Sigma-Aldrich Company, (USA). Dichlorodiphenylsilane (Ph_2Cl_2Si) was purchased from Beijing Coupling Technology Company Ltd, (China). 2,2'-Bis(diphenylphosphino)-1,1'-binaphthyl ((R)-BINAP) was obtained from Shijiazhuang Shengjia Chemical Co, Ltd., (China). Tetraethoxysilane (TEOS) was purchased from Shanghai Chemical Reagent Company of the Chinese Medicine Group. Methyl acetoacetate and other β-keto esters were purchased from Alfa Aesar Company. All of the solvents were of analytical quality and deoxygenated by standard methods before being used.

Preparation methods

Ru-(*R*-Binap) complex was synthesized according to the literature method and was fully characterized by FT-IR (Figure 2a), UV-vis (Figure S3), ^{31}P-NMR (Figure 4), ^{1}H-NMR and ^{13}C-NMR spectroscopy (Figures S1~S3).[32]

The mesoporous material FDU-12 was synthesized according to the literature method.[34] C-FDU-12 was obtained by carbonization of the as-made FDU-12 at 550 °C under the nitrogen atmosphere for 6 h.

The encapsulation was performed in the glove-box. A typical process for the encapsulation of Ru-(*R*-Binap) in the nanocages of C-FDU-12 was as follows: C-FDU-12 (0.2 g) evacuated at room temperature for 0.5 h. CH_2Cl_2 (0.5 mL) containing a given number of Ru-(*R*-Binap) was injected into

C-FDU-12 material under a vacuum condition with vigorous stirring. After evaporation of CH_2Cl_2, 1 ml of dry hexane was injected into the resultant solid, followed with 0.5 ml of Ph_2Cl_2Si (12mmol/g). After reaction for 8 h under this low pressure and room temperature, the resulting solid catalyst was isolated by filtration and thoroughly washed with CH_2Cl_2. The Ru content of the encapsulated catalysts varied from 0.12 to 0.82 wt%. The number of Ru-(*R*-Binap) in each cage (n, Table 2) was calculated by the following equation:

$$n = \frac{N_{Ru(1g)} \times 6.02 \times 10^{23}}{\frac{V_{meso}}{\frac{4}{3}\pi(\frac{D}{2})^3}}$$

$N_{Ru(1g)}$ is the mole of Ru-(*R*-Binap) per gram of the solid catalyst.

$V_{meso.} = V_{total} - V_{microp.}$, where V_{total} means the total pore volume, $V_{meso.}$ refers to the pore volume attributed by the mesopore and $V_{microp.}$ refers to the pore volume of the micropore.

D is cage size of C-FDU-12.

Asymmetric hydrogenation of β-keto esters

A desired amount of homogeneous or heterogeneous Ru-(*R*-Binap) catalyst (2 umol) was added in a ampoule tube, followed by the addition of β-keto esters (2 mmol) and anhydrous methanol (1 mL). The ampoule tube was then transferred into a stainless steel autoclave and sealed. After purging with H_2 for six times, the final H_2 pressure was adjusted to 4 MPa, and the reactor was heated to 323 K whilst vigorous stirring (700 rpm) for 24 h. After cooling down to room temperature, H_2 pressure in the autoclave was released. The solid catalyst was separated by centrifugalization and washed with 4 ml of MeOH. The filtration was collected and analyzed by an Agilent 6890 GC equipped with a chiral Supelco γ-DEX 225 capillary column (30 m×0.25 mm×0.25μm). The GC spectra of the corresponding products hydrogenated by various β-keto esters were given in the supporting information (Figure S4).

For recycling the catalyst, the autoclave was opened in the glove box. After centrifugation under N_2, the liquid was decanted, and the residual catalyst was washed thoroughly with CH_2Cl_2, dried under vacuum and used directly for the next catalytic reaction.

Characterization

N_2 sorption isotherms were carried out on a Micromeritics ASAP2020 volumetric adsorption analyzer. Before the sorption measurements, samples were out gassed at 393 K for 6 h. X-Ray powder diffraction (XRD) patterns were recorded on a Rigaku RINT D/Max-2500 powder diffraction system using Cu Kα radiation (λ=0.1541 nm). Transmission electron microscopy (TEM) was performed using a FEI Tecnai G2 Spirit at an acceleration voltage of 120 kV. FT-IR spectra were collected with a Nicolet Nexus 470 IR spectrometer. All liquid and solid ^{31}P-NMR spectroscopy experiments were carried out at 9.4 T on a Varian Infinity Plus 400 spectrometer with a ^{31}P frequency of 161.83 MHz using a 5 mm Chemagnetic probe. One pulse sequence was used to collect ^{31}P liquid and solid NMR data, using π/2 pulse width of 1.9 us and the recycle delay of 10 s. The spinning rates in solid NMR experiments are 6 kHz and 7 kHz. The chemical shifts were referenced to $(NH_4)_2HPO_4$.

Ru-(*R*-Binap) (100mg) in dried form was measured by ^{31}P MAS and static NMR. With the addition of different volumes of $CHCl_3$ (5 uL to 300 uL), the sample was kept for 30 min and detected by ^{31}P static NMR.

Acknowledgements

The authors would like to thank the financial support of the Natural Science Foundation of China (21325313, 21232008 and 21273226).

Notes and references

[a] State Key Laboratory of Catalysis, Dalian Institute of Chemical Physics, Chinese Academy of Sciences, 457 Zhongshan Road, Dalian 116023, China, Fax: (+86)0411-84694447, E-mail: yangqh@dicp.ac.cn, canli@dicp.ac.cn

[b] Graduate School of the Chinese Academy of Sciences
Beijing 100049, China

1 Z. J. Jia, K. Jiang, Q. Q. Zhou, L. Dong, Y. C. Chen, *Chem. Commun.* 2013, **49**, 5892-5894.
2 J. H. Wang, D. L. Liu, Y. G. Liu, W. B. Zhang, *Org. Biomol. Chem.* 2013, **11**, 3855-3861.
3 A. E. Sheshenev, E. V. Boltukhina, A. J. P. White, K. K. Hii, *Angew. Chem. Int. Ed.* 2013, **52**, 6988-6991.
4 S. K. Murphy, V. M. Dong, *J. Am. Chem. Soc.* 2013, **135**, 5553-5556.
5 K. Li, N. F. Hu, R. S. Luo, W. C. Yuan, W. J. Tang, *J. Org. Chem.* 2013, **78**, 6350-6355.
6 S. Xiang, Y. L. Zhang, Q. Xin, C. Li, *Chem. Commun.* 2002, 2696-2697.
7 P. Piaggio, P. McMorn, C. Langham, D. Bethell, P. C. Bulman, F. E. Hancock, G. J. Hutchings, *New J. Chem.*1998, **22**, 1167-1169.
8 N. Herron,*Inorg. Chem.* 1986, **25**, 4714-4717.
9 M. J. Sabater, A. Corma, A. Domenech, V. Fornes, H. Garcia, *Chem. Commun.* 1997, 1285-1286.
10 A. Corma, H. Garcia, *Eur. J. Inorg. Chem.* 2004, 1143-1164.
11 H. Q. Yang, L. Zhang, L. Zhong, Q. H. Yang, C. Li,*Angew. Chem. Int. Ed.* 2007, **46**, 6861-6865.
12 H. Q. Yang, J. Li, J. Yang, Z. M. Liu, Q. H. Yang, C. Li, *Chem. Commun.* 2007, 1086-1088.
13 B. Li, S. Y. Bai, X. F. Wang, M. M. Zhong, Q. H. Yang, C. Li, *Angew. Chem. Int. Ed.* 2012, **51**, 11517-11521.
14 H. Q. Yang, L. Zhang, P. Wang, Q. H. Yang, C. Li,*Green Chem.*2009, **11**, 257-264.
15 B. Li, S. Y. Bai, P. Wang, H. Q. Yang, Q. H. Yang, C. Li, *Phys. Chem. Chem. Phys.* 2011, **13**, 2504-2511.
16 S. Y. Bai, B. Li, J. Peng, X. M. Zhang, Q. H. Yang, C. Li, *Chem. Sci.* 2012, **3**, 2864-2867.
17 S. Y. Bai, H. Q. Yang, P. Wang, J. S. Gao, B. Li, Q. H. Yang, C. Li, *Chem. Commun.* 2010, **46**, 8145-8147.
18 X. Liu, S. Y. Bai, Y. Yang, B. Li, B. Xiao, C. Li, Q. H. Yang, *Chem. Commun.* 2012, **48**, 3191-3193.

19 A. Miyashita, H. Takaya, K. Toriumi, T. Ito, T. Souchi, R. Noyori, *J. Am. Chem. Soc.* 1980, **102**, 7932-7934.
20 A. G. Hu, H. L. Ngo, W. B. Lin, *J. Am. Chem. Soc.* 2003, **125**, 11490-11491.
21 A. G. Hu, H. L. Ngo, W. B. Lin, *Angew. Chem. Int. Ed.* 2003, **42**, 6000-6003.
22 A. G. Hu, S. Liu, W. B. Lin, *RSC. Adv.*2012, **2**, 2576-2580.
23 A. G. Hu, G. T. Yee, W. B. Lin, *J. Am. Chem. Soc.* 2005, **127**, 12486-12487.
24 P. Y. Wang, X. Liu, J. Yang, Y. Yang, L. Zhang, Q. H. Yang, C. Li, *J. Mater. Chem.* 2009, **19**, 8009-8014.
25 A. B. Dongil, B. Bachiller-Baeza, A. Guerrero-Ruiz, I. Rodriguez-Ramos, *Catal.Commun.* 2012, **26**, 149-154.
26 Q. Sun, X. J. Meng, X. Liu, X. M. Zhang, Y. Yang, Q. H. Yang, F. S. Xiao, *Chem. Commun.* 2012, **48**, 10505-10507.
27 A. L. Monteiro, F. K. Zinn, R. F. deSouza, J. Dupont, *Tetrahedron: Asymmetry*1997, **8**, 177-179.
28 T. Floris, P. Kluson, L. Bartek, H. Pelantova, *Appl. Catal. A: General* 2009, **366**, 160-165.
29 J. Theuerkauf, G. Francio, W. Leitner, *Adv. Synth. Catal.* 2013, **355**, 209-219.
30 T. Deschner, Y. C. Liang, R. Anwander, *J. Phys. Chem. C* 2010, **114**, 22603-22609.
31 J. Fan, C. Z. Yu, J. Lei, Q. Zhang, T. C. Li, B. Tu, W. Z. Zhou, D. Y. Zhao, *J. Am. Chem. Soc.* 2005, **127**, 10794-10795.
32 M. Kitamura, T. Ohkuma, R. Noyori, *Org. Synth., Coll. Vol.*1998, **9**, 589.
33 A. R. McDonald, C. Muller, D. Vogt, G. P. M. van Klink, G. van Koten, *Green Chem.* 2008, **10**, 424-432.
34 J. Fan, C. Z. Yu, F. Gao, J. Lei, B. Z. Tian, L. M. Wang, Q. Luo, B. Tu, W. Z. Zhou, D. Y. Zhao, *Angew. Chem. Int. Ed.* 2003, **42**, 3146-3150.

Ru-(*R*-Binap) encapsulated in silica-based nanoreactors: a solid catalyst as a whole, but a homogeneous catalyst at nanoscale.